DETECTION OF BROKEN ROTOR BAR FAULTS IN INDUCTION MOTOR BY SPECTRUM ANALYSIS

S.M.Shashidhara
Professor
Dept of EEE, RYM Engineering College, Ballari, India

***Abstract*— A broken bar might cause a number of effects in induction motors. The manifestation of the sideband components is one of the frequent effects of a broken bar. The sideband components can be found in the power spectrum of the stator current on left and right sides of the fundamental frequency component. The left side band constituent is caused due to electromagnetic asymmetries in the rotor cage and on the other hand, the right sideband component is generated because of resulting speed ripples caused due to resultant pulsations in torque. Analyzing the spectral components of the motor induced signals is the most common signal processing based method employed for fault diagnosis and condition monitoring of induction motors. The fault 'finger prints' are unique and can be easily recognised in the spectrum analysis.**

***Keywords*— Fast Fourier Transform, Induction Motor, Broken Rotor Fault, MCSA, Fault frequency components**

1 Introduction

The design and manufacturing of squirrel-cage rotor have undergone small changes over decades. Faults associated with the rotor are generally related to thermal stresses, magnetic stresses, and stresses due to inadequate manufacturing, and environmental stresses that are caused by moisture [1]. The inception of rotor faults starts with the higher resistance resulting into the higher heat generation and then grows into cracks or holes in the rotor bars [2]. These faults are more likely to take place at the end rings.

Various parameters such as pulsations in the motor speed, vibration, air-gap flux and motor current can be monitored for the diagnosis of broken rotor bars. Early fault detection techniques can notably reduce maintenance costs for these motors. The condition monitoring aims at fault diagnosis in electric motors. The spectral analysis techniques are considered as one of the important techniques in the literature [3,4].

A number of researchers have carried out the approach of motor current spectrum evaluation for fault detection. Researches like [5-7] employed the motor current signature analysis (MCSA) approach for detecting the faults in broken rotor bars. In their work, they established sideband components around the fundamental frequency to detect broken bar faults. The fault in rotor bars is emulated with artificially drilled holes in the bars in such a way that the holes cut the bars completely. (Figure 4.1).

The lower sideband is unique to a broken bar, while the upper sideband is a upshot of the oscillation in speed. The variable f_s represents the frequency of the phase current and other parameters, 's' refers to the motor slip with k as constant k = 0, 1, 2,..., n.

$$f_{br} = (1 \pm 2ks) f_s \quad (1)$$

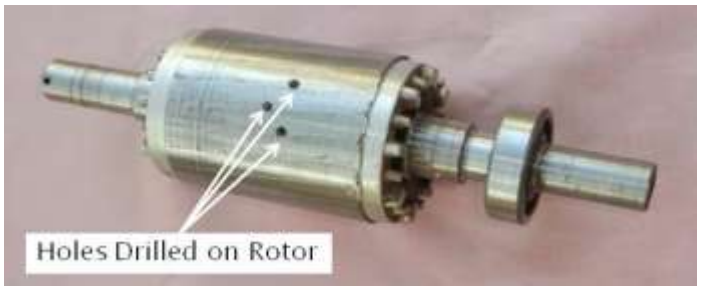

Figure 1 Fault created by drilling holes on rotor bars

There is a proportionate change in the magnitude of sideband frequency as per the change in the load inertia. Moreover, the other spectral components, which take place, can be acquired from the line current of the motor with the application of equation mentioned above [8]. Figure 2 depicts the ideal current spectrum for frequency analysis. f_s is the supply frequency and lower and upper side band components are also shown.

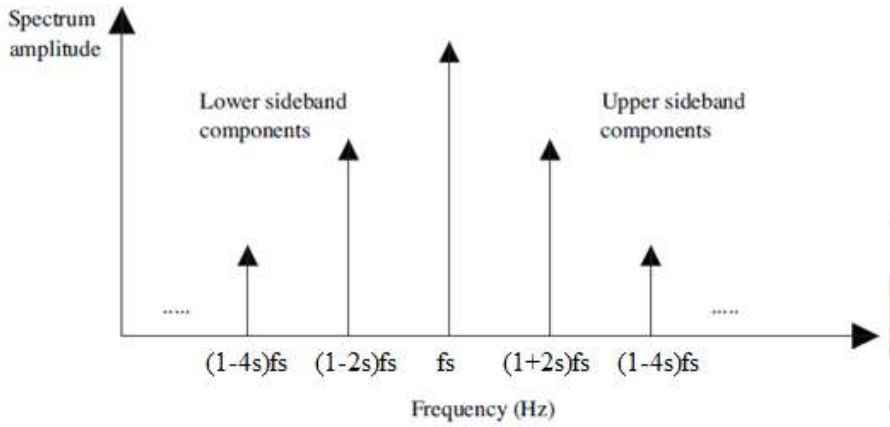

Figure 2 Ideal Current spectrum

2 Spectrum Analysis using LabVIEW

In this work, interfacing between devices has been developed for observing and ultimately accomplishing the fault detection and diagnosis in broken rotor bars. In order to get the data from the machineries, a data acquisition device from National Instruments™ LabVIEW ('Laboratory Virtual Instrument Engineering Workbench') has been employed.

2.1 Data Acquisition device

NI USB-6008 Data Acquisition device: The NI USB-6008 (National Instruments) data acquisition device was used to record real diagnostic signals originating from the instrument panel installed at the laboratory. The NI USB-6008 data acquisition device is shown in Fig 4. This data acquisition device is equipped with 8 single analogue inputs (or 4 differential programmable analogue inputs), 2 analogue outputs and 12 programmable digital I/O systems. The information received from the input or output control signals are sent to thecontrol unit (a PC) through a USB connection. The signal transmitted between the data acquisition device and the PC conforms to full speed USB standards [9]. The data acquisition device NI USB-6008 has been shown in Figure 3 (a).

NI myDAQ was also employed in the place of USB-6008, for similar test benches and experiments, which is shown in Figure 3(b). NI myDAQ is a data acquisition (DAQ) device that gives the ability to measure and analyse live signals. myDAQ includes two analog inputs and two analog outputs at 200 kS/s and 16 bits, allowing for applications such as sampling a sensor output signal; eight digital inputs and output lines. In this experiment a scan rate of 2kS/s was selected.

(a) (b)

Figure 3 Data acquisition devices (a) NI USB-6008 (b) NI myDAQ

Figure 4 shows the framework of data acquisition and analysis system. It comprises of a current sensor signal given as input to DAQ and PC for data visualization.

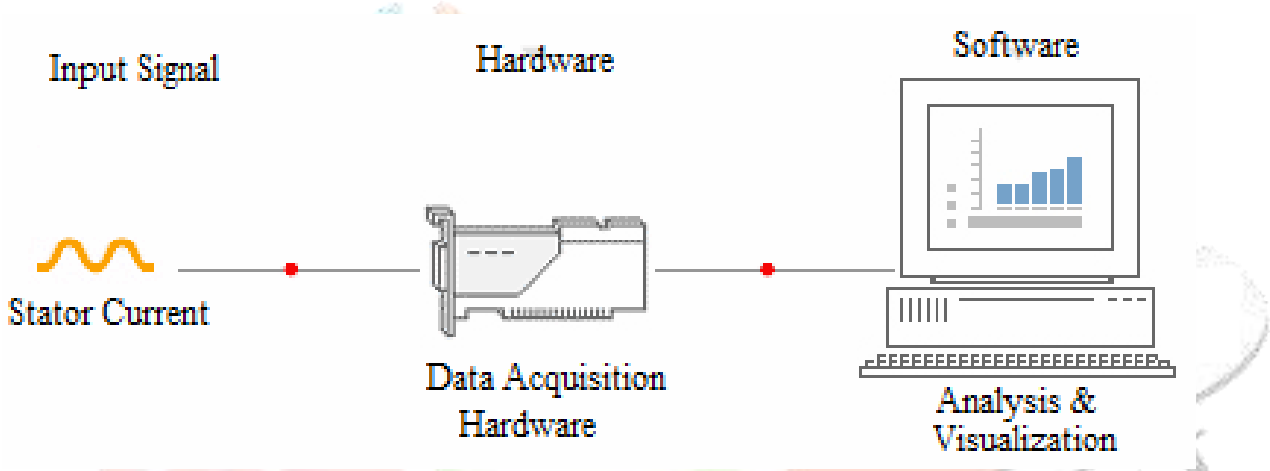

Figure 4 Framework of data acquisition and analysis

A Hall effect sensor WCS2705 was used to isolate the motor phase current signal with a sensitivity of 255mV/A. Applied current flowing though the sensor generates a magnetic field which is sensed by the integrated IC and converted to a proportional voltage.

Tests were conducted for different loads with the healthy motor and with similar motors having up to 4 broken rotor bars. The rotor faults were created by breaking the rotor bars by drilling holes into the rotor ensuring that, rotor bar is cut completely. The measured current signals were processed using the Fast Fourier Transformation (FFT) spectrum analysis through Virtual Instrumentation. The results obtained for the healthy motor and those having rotor broken bar faults were compared, especially looking for the sideband components.

The motor was coupled with a mechanical load to accomplish the detection of fault at various loading conditions. In the experimental analysis process, the rated data of the machine selected for system realization are as given in Table 1. Experimental setup is shown in Figure 5, flowchart of LabVIEW based DAQ in Figure 6 and VI panel is presented in Figure 7.

Figure 5 Experimental setup

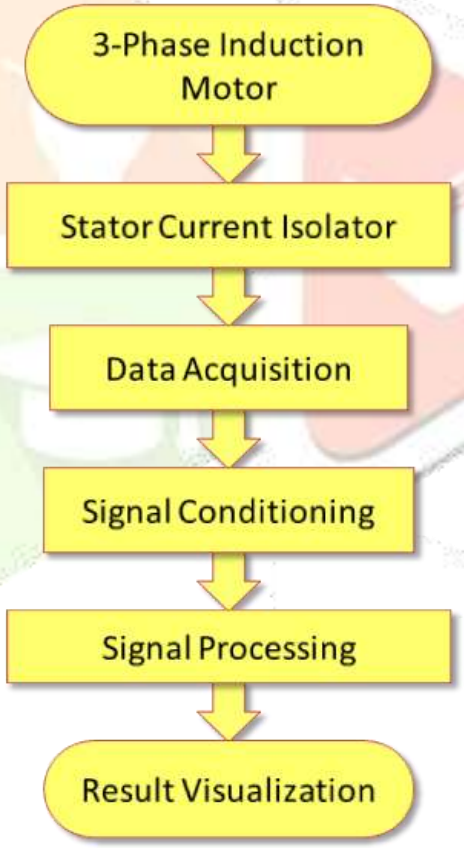

Figure 6 flowchart of LabVIEW based DAQ

Table 1 Motor specifications

Component	Specification
Induction motor	3-Phase Squirrel-Cage Induction Motor
Voltage rating(rms)	415 V
Current rating	1.8 Amp
Operation Frequency	50Hz
Power rating	1 HP
No. of Poles	4

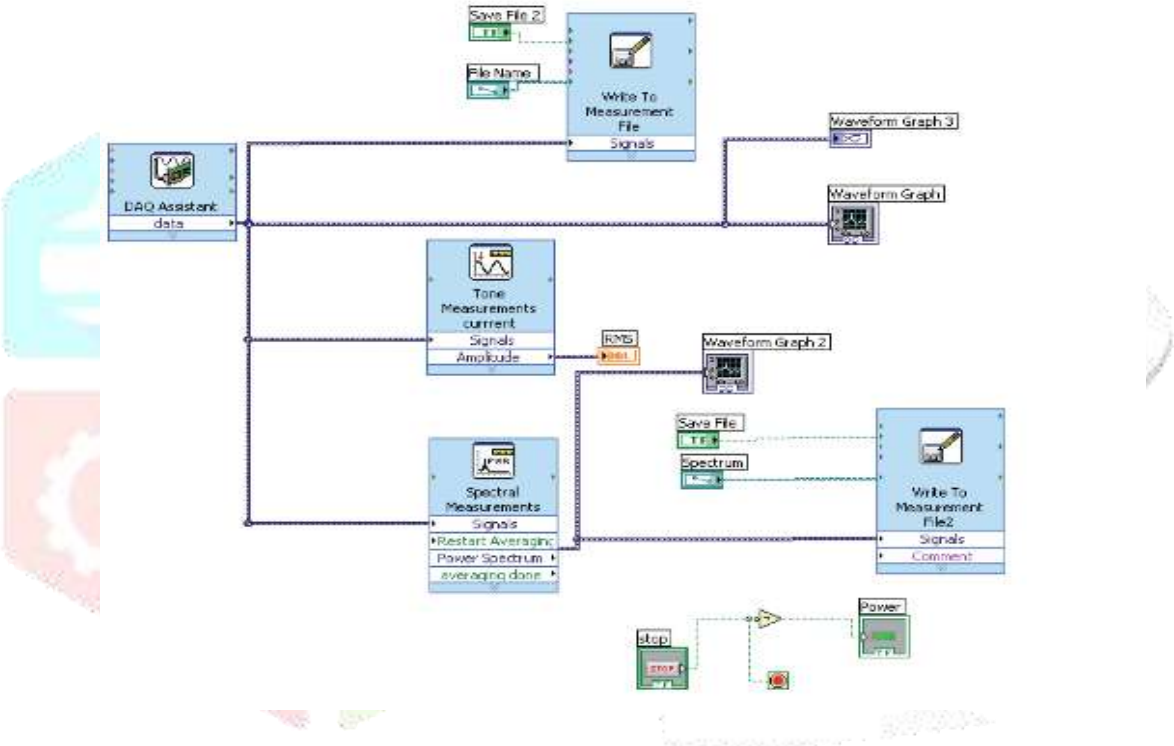

Figure 7 Block diagram of the developed Virtual Instrument Panel

3. RESULTS

As these sideband frequencies are functions of the slip, they are changing with the speed (implicitly with the load). This phenomenon can be distinctly observed from Figure 8 (a) to (c), where the power spectral density of the measured currents for the motor having 4 broken bars are plotted for three different cases. As it can be ascertained, the magnitude of the sideband frequency constituents is also increasing as the load is increased.

As already stated, the presence of the slip frequency sidebands establishes the existence of the broken rotor bars. The magnitude is the function of the number of the broken bars. This can be ascertained by referring to the Table 2 in which, amplitudes of fault frequency components for healthy and faulty motors are given. Figure 9 shows the variation of fault frequencies and their amplitudes with the number of broken rotor bars. It is evident from the plot that the number of broken bars can be found out through the measurement of fault frequencies and their amplitudes.

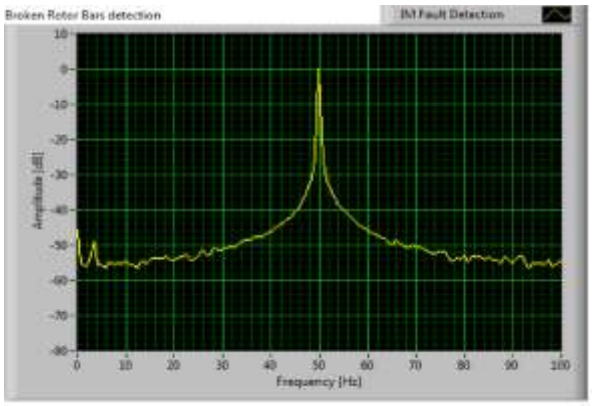

(a) Current spectrum in healthy motor at No-load

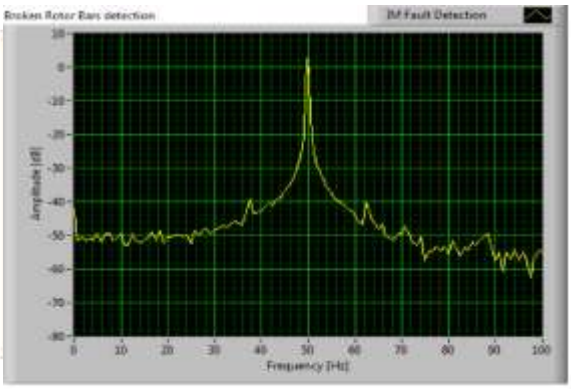

(b) Current spectrum in faulty state motor at half-load

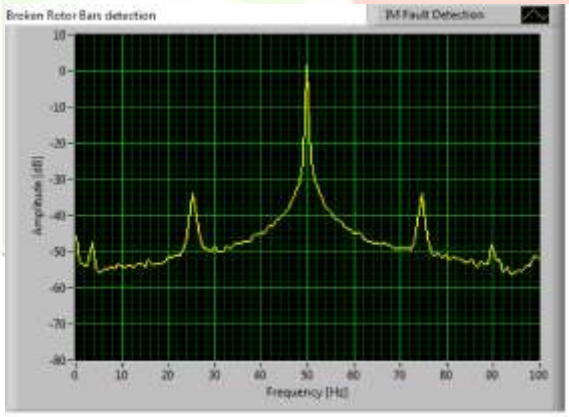

(c) Current spectrum in faulty state motor at full-load

Figure 8 current spectrums for 4 broken bars

Table 2 Amplitudes of fault frequency components for healthy and faulty motors

No. of BRBs	LSB Frequency	USB Frequency	Amplitude of LSB Frequencies	Amplitude of LSB Frequencies
0	49	51	-52	-52
1	44	56	-48	-48
2	40	60	-44	-44
3	33	67	-38	-38
4	28	72	-34	-34

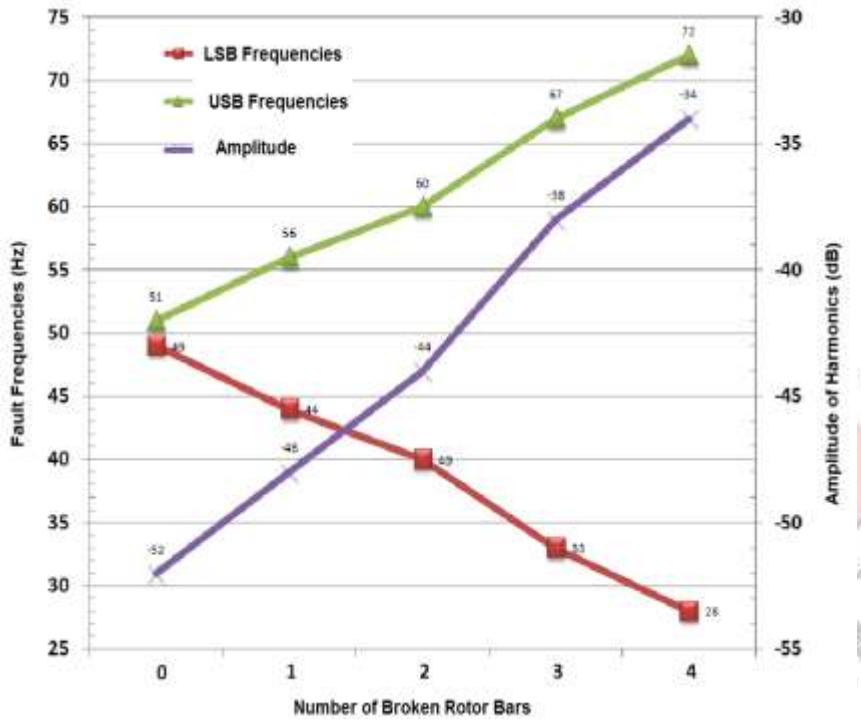

Figure 9 Variation of fault frequencies and their amplitudes with the number of broken rotor bars

4. CONCLUSIONS

In this paper, a system for fault identification in rotor bars of induction motors was developed. Experimental investigations were conducted. From the huge number of obtained results here only the most significant ones are presented. In this study, the major parts of interest are the effects of the broken rotor bar fault on motor stator current spectrum under healthy and faulty conditions. The current spectrums obtained from the current signal for four broken bars at no load and with load are given in Figures 8. At no load condition, the side band frequencies are close to fundamental frequency and the amplitudes of the sidebands are almost negligible. The

detection of the slip frequency sideband at no load or light load is quite difficult. Figures 8 (b) and (c) show the current spectrum component of motor with four broken bars under load condition. It is observed from the figure that broken bar fault detection at load performed in more reliable way. The frequency components related to broken bar can be quite clearly recognized in the current spectrum.

REFERENCES

[1] S. Nandi, H.A. Toliyat, X. Li, "Condition monitoring and fault diagnosis of electrical motors -a review," *IEEE Transactions on Energy Conversion*, Vol. 20, pp. 719-729, 2005.

[2] Çalış, Hakan, and Abdülkadir Çakır. "Rotor bar fault diagnosis in three-phase induction motors by monitoring fluctuations of motor current zero crossing instants." *Electric power systems Research*, no. 5, 385-392, 2007.

[3] S. Seker, "Determination of air gap eccentricity in electric motors using coherence analysis," *IEEE Power Engineering Review*, Vol. 20, pp.48-50, 2000.

[4] S. Seker, E. Ayaz, "Feature extraction related to bearing damage in electric motors by wavelet analysis," *Journal of the Franklin Institute*, Vol. 340, pp. 125-134, 2003.

[5] G.B. Kliman, R.A. Koegl, J. Stein, R.D. Endicott, M.W. Madden, "Non-invasive detection of broken rotor bars in operating induction motors," IEEE Transactions on Energy Conversion, Vol. 3, pp. 873-879, 1988.

[6] F. Filippetti, G. Franceschini, C. Tassoni, P. Vas, "AI techniques in induction machines diagnosis including the speed ripple effect," IEEE Industry Applications Society Annual Meeting Conference, pp. 655-662, 1996.

[7] Siddiqui, Khadim Moin, Kuldeep Sahay, and V. K. Giri. "Health Monitoring and Fault Diagnosis in Induction Motor-A Review," *International Journal of Advanced Research in Electrical, Electronics and Instrumentation Engineering*, Vol. 3, Issue 1, January 2014

[8] M. Haji, H.A. Toliyat, "Pattern recognition - a technique for induction machines rotor broken bar detection," *IEEE Transactions on Energy Conversion*, Vol. 16, pp. 312-317, 2001.

[9] S.M. Shashidhara and Dr.P.Sangameswara Raju, Diagnosis of Broken Rotor Bars in Induction Motor by Using Virtual Instruments. International Journal of Electrical Engineering and Technology (IJEET), 4(5), 2013, pp. 78–86